

## Central Lancashire Online Knowledge (CLoK)

Title	Effect of mechanical denaturation on surface free energy of protein powders
Type	Article
URL	<a href="https://clock.uclan.ac.uk/15855/">https://clock.uclan.ac.uk/15855/</a>
DOI	##doi##
Date	2016
Citation	Mohammad, Mohammad Amin, Grimsey, Ian M., Forbes, Robert Thomas orcid iconORCID: 0000-0003-3521-4386, Blagbrough, Ian S. and Conway, Barbara R (2016) Effect of mechanical denaturation on surface free energy of protein powders. Colloids and Surfaces B: Biointerfaces, 146 . pp. 700-706. ISSN 0927-7765
Creators	Mohammad, Mohammad Amin, Grimsey, Ian M., Forbes, Robert Thomas, Blagbrough, Ian S. and Conway, Barbara R

It is advisable to refer to the publisher's version if you intend to cite from the work. ##doi##

For information about Research at UCLan please go to <http://www.uclan.ac.uk/research/>

All outputs in CLoK are protected by Intellectual Property Rights law, including Copyright law. Copyright, IPR and Moral Rights for the works on this site are retained by the individual authors and/or other copyright owners. Terms and conditions for use of this material are defined in the <http://clock.uclan.ac.uk/policies/>

1                   **Effect of mechanical denaturation on surface free energy of protein powders**

2                   Mohammad Amin Mohammad<sup>a,b\*</sup>, Ian M. Grimsey<sup>a</sup>, Robert T. Forbes<sup>a</sup>

3                   Ian S. Blagbrough<sup>c</sup>, and Barbara R Conway<sup>d</sup>

4                   <sup>a</sup> School of Pharmacy, University of Bradford, Bradford, BD7 1DP, UK.

5                   <sup>b</sup> Faculty of Pharmacy, University of Damascus, Damascus, Syria.

6                   <sup>c</sup> Department of Pharmacy and Pharmacology, University of Bath, Bath BA2 7AY, UK.

7                   <sup>d</sup> Department of Pharmacy, University of Huddersfield, Queensgate, Huddersfield, HD1 3DH,  
8 UK.

9  
10  
11 \* Corresponding author

12 Dr. Mohammad Amin Mohammad

13 Associate Professor in Pharmaceutical Technology

14 First name: Mohammad Amin

15 Family name: Mohammad

16 Phone: + 44 (0)1225 386797

17 Email: [m.a.mohammad7@bradford.ac.uk](mailto:m.a.mohammad7@bradford.ac.uk)

18 Postal address: Dr. Mohammad Amin Mohammad, School of Pharmacy, University of Bradford,  
19 Richmond Road, Bradford, BD7 1DP, UK.

20  
21 Dr. Ian M. Grimsey, Senior Lecturer in Pharmaceutical Technology

22 Phone: +44 (0)1274 234754

23 Email: [i.m.grimsey@bradford.ac.uk](mailto:i.m.grimsey@bradford.ac.uk)

24 School of Pharmacy, University of Bradford, Bradford BD7 1DP, UK

25  
26 Prof. Robert T. Forbes, Professor of Biophysical Pharmaceutics

27 Phone: +44 (0)1274 234653

28 Email: [r.t.forbes@bradford.ac.uk](mailto:r.t.forbes@bradford.ac.uk)

29 School of Pharmacy, University of Bradford, Bradford BD7 1DP, UK

30  
31 Dr. Ian S. Blagbrough

32 Phone: +44 (0) 1225 386795

33 Email: [prsisb@bath.ac.uk](mailto:prsisb@bath.ac.uk)

34 Department of Pharmacy and Pharmacology, University of Bath, Bath BA2 7AY, UK.

35  
36 Prof. Barbara R Conway,

37 Phone: +44 (0) 1484 472347

38 Email: [b.r.conway@hud.ac.uk](mailto:b.r.conway@hud.ac.uk)

39 Department of Pharmacy, University of Huddersfield, Queensgate, Huddersfield, HD1 3DH, UK.  
40  
41  
42  
43  
44  
45

46 **ABSTRACT**

47 Globular proteins are important both as therapeutic agents and excipients. However, their fragile  
48 native conformations can be denatured during pharmaceutical processing, which leads to  
49 modification of the surface energy of their powders and hence their performance. Lyophilized  
50 powders of hen egg-white lysozyme and  $\beta$ -galactosidase from *Aspergillus oryzae* were used as  
51 models to study the effects of mechanical denaturation on the surface energies of basic and acidic  
52 protein powders, respectively. Their mechanical denaturation upon milling was confirmed by the  
53 absence of their thermal unfolding transition phases and by the changes in their secondary and  
54 tertiary structures. Inverse gas chromatography detected differences between both unprocessed  
55 protein powders and the changes induced by their mechanical denaturation. The surfaces of the  
56 acidic and basic protein powders were relatively basic, however the surface acidity of  $\beta$ -  
57 galactosidase was higher than that of lysozyme. Also the surface of  $\beta$ -galactosidase powder had a  
58 higher dispersive energy compared to lysozyme. The mechanical denaturation decreased the  
59 dispersive energy and the basicity of the surfaces of both protein powders. The amino acid  
60 composition and molecular conformation of the proteins explained the surface energy data  
61 measured by inverse gas chromatography. The biological activity of mechanically denatured  
62 protein powders can either be reversible (lysozyme) or irreversible ( $\beta$ -galactosidase) upon  
63 hydration. Our surface data can be exploited to understand and predict the performance of protein  
64 powders within pharmaceutical dosage forms.

65

66 *Keywords:*

67 Protein denaturation;  $\beta$ -Galactosidase; Lysozyme; Conformational change; Inverse gas  
68 chromatography; Surface free energy.

69 **1. Introduction**

70

71 In the pharmaceutical field, there is considerable interest in the use of globular proteins for  
72 their therapeutic effects. During pharmaceutical processes, protein powders are often subjected to  
73 mechanical stresses. For example, milling has been used to prepare protein particles suitable for  
74 pulmonary delivery and protein-loaded microparticles in industrial quantities [1,2]. The  
75 mechanical stresses applied during the milling can partially or completely denature the proteins  
76 and change their bulk properties [3]. In recent years, denatured globular proteins have found  
77 extensive applications as excipients in pharmaceutical formulations [4,5]. Denatured globular  
78 proteins have been used to prepare emulsion systems designed to enhance the absorption of  
79 insoluble drugs and to form nanoparticles for drug delivery and targeting [4]. Globular proteins  
80 have also been successfully used to formulate controlled drug delivery tablets, which delay drug  
81 release in gastric conditions by forming a gel-layer stabilized by intermolecular- $\beta$  sheets of  
82 denatured globular proteins [5].

83 Surface energies of powders are critical properties to be considered during formulation and  
84 development of dosage forms in the pharmaceutical industry. Surface energy has significant effects  
85 on pharmaceutical processes such as granulation, tableting, disintegration, dissolution,  
86 dispersibility, immiscibility, wettability, adhesion, flowability, packing etc. Resultant data from  
87 recent determination of surface energies have been used to reduce the time of formulation  
88 development and enhance the quality of the final product [6-8].

89 The effect of the protein denaturation on their surface chemistry has been determined using  
90 time-of-flight secondary ion mass spectrometry [9]. However, the effect of mechanical  
91 denaturation on the surface energies of globular proteins has not been reported and these effects

92 must be understood to exploit the full potential of globular proteins in pharmaceutical industry  
93 both as therapeutic agents and excipients. Inverse gas chromatography (IGC) is a useful verified  
94 tool for surface energy measurements [10]. IGC has been used to measure the surface free energy  
95 of lyophilized protein particles, detecting lot-to-lot variations in the amorphous microstructure of  
96 lyophilized protein formulations [11].

97         This paper aims to evaluate the effects of mechanical denaturation on the surface energies  
98 of globular protein powders using IGC.  $\beta$ -Galactosidase is a hydrolytic enzyme that has been  
99 widely investigated for potential applications in the food industry to improve sweetness, solubility,  
100 flavor, and digestibility of dairy products. Preparations of  $\beta$  galactosidases have also been  
101 exploited for industrial, biotechnological, medical, and analytical applications [12]. Lysozyme is  
102 a naturally occurring enzyme found in bodily secretions such as tears, saliva, and milk and has  
103 been explored as a food preservative and pharmaceutical. The isoelectric points (pI) of  $\beta$ -  
104 galactosidase from *Aspergillus oryzae* and hen egg-white lysozyme are 4.6 and 11.3, and were  
105 used as models of acidic and basic globular proteins, respectively [13]. Lyophilized powders of  
106 these proteins were mechanically denatured by milling. Their surface energies before and after  
107 denaturation were compared in order to understand how the surfaces of the globular protein  
108 powders respond to the mechanical denaturation.

109

## 110 **2. Materials and methods**

### 111 *2.1. Materials*

112         *Micrococcus lysodeikticus* (Sigma-Aldrich), 2-nitrophenyl  $\beta$ -D-galacto pyranoside  
113 (Sigma-Aldrich), lyophilized powders of  $\beta$ -galactosidase from *A. oryzae* (Sigma-Aldrich) and hen  
114 egg-white lysozyme (Biozyme Laboratories, UK) were purchased as indicated. The purchased  $\beta$ -

115 galactosidase and lysozyme powders were considered to be unprocessed samples and named UNG  
116 and UNL, respectively.

117

## 118 *2.2. Preparation of mechanically denatured protein powders*

119 Mechanically denatured powders of  $\beta$ -galactosidase and lysozyme were prepared by  
120 manually milling. The milling was achieved by rotating a marble pestle over the powder within a  
121 marble mortar at ~45 cycles per minute (cpm). Milling times of 60 min were enough to completely  
122 denature the protein powders, and this was confirmed by differential scanning calorimetry (DSC)  
123 [3]. The mechanically denatured powders of  $\beta$ -galactosidase and lysozyme were named DeG and  
124 DeL, respectively. Three batches (2 g each batch) of the mechanically denatured powders were  
125 prepared for each protein.

126

## 127 *2.3. Microscopy*

128 A Zeiss Axioplan2 polarizing microscope (Carl Zeiss Vision GmbH; Hallbergmoos,  
129 Germany) was used to visualize the samples. The accompanying software (Axio Vision 4.2) was  
130 then used to determine the projected area diameters of the powders.

131

## 132 *2.4. Differential scanning calorimetry (DSC)*

133 Differential scanning calorimetry (DSC) thermograms were obtained using a Perkin-Elmer  
134 Series 7 DSC (Perkin-Elmer Ltd., Beaconsfield, UK). Samples (4-7 mg) were sealed in aluminium  
135 pans. The escape of water was facilitated by making a pinhole in the lid prior to sealing. The  
136 samples were equilibrated at 25 °C and heated to 250 °C at a scan heating rate of 10 °C/min under  
137 a flow of anhydrous nitrogen (20 ml/min). Each sample was analysed in triplicate. The temperature

138 axis and cell constant of the DSC cell were calibrated with indium (10 mg, 99.999 % pure, melting  
139 point 156.60 °C, and heat of fusion 28.40 J/g).

140

#### 141 2.5. FT-Raman spectroscopy

142 FT-Raman spectra of samples were recorded with a Bruker IFS66 optics system using a  
143 Bruker FRA 106 Raman module. The excitation source was an Nd: YAG laser operating at 1064  
144 nm and a laser power of 50 mW was used. The FT-Raman module was equipped with a liquid  
145 nitrogen cooled germanium diode detector with an extended spectrum band width covering the  
146 wave number range 1800-450  $\text{cm}^{-1}$ . Samples were placed in stainless steel sample cups and  
147 scanned 200 times with the resolution set at 8  $\text{cm}^{-1}$ . The observed band wave numbers were  
148 calibrated against the internal laser frequency and are correct to better than  $\pm 1 \text{ cm}^{-1}$ . The spectra  
149 were corrected for instrument response. The experiments were run at a controlled room  
150 temperature of  $20 \pm 1 \text{ }^\circ\text{C}$ .

151

#### 152 2.6. Enzymatic assay

153 The enzymatic activity of lysozyme samples was measured to determine the ability of  
154 lysozyme to catalyze the hydrolysis of  $\beta$ -1,4-glycosidic linkages of cell-wall mucopolysaccharides  
155 [14]. Lysozyme solution (30  $\mu\text{l}$ , 0.05 % in phosphate buffer, pH = 5.2; 10 mM) was added to  
156 *Micrococcus lysodeikticus* suspension (2.97 ml, 0.025 % in phosphate buffer, pH = 6.24; 66 mM).  
157 The decrease in the absorbance at 450 nm was monitored by using a UV-Vis spectrophotometer  
158 (PU 8700, Philips, UK). The activity was determined by measuring the decrease in the substrate  
159 bacterial suspension concentration with time. Hence the slope of the reduction in light absorbance  
160 at 450 nm against the time of 3 min, starting when the protein solutions were mixed with the

161 substrate bacterial suspension, was considered to be the indicator of the lytic activity of lysozyme  
162 [15].

163 The enzymatic activity of  $\beta$ -galactosidase samples was determined using a method relying  
164 on the ability of  $\beta$ -galactosidase to hydrolyse the chromogenic substrate *o*-nitrophenyl  $\beta$ -D-galacto  
165 pyranoside (ONPG) to *o*-nitrophenol [16]. The results were achieved by adding 20  $\mu$ l of protein  
166 solution (0.05 w/v% in deionised water) to 4 ml of the substrate solution (0.665 mg/ml) in a  
167 phosphate buffer (100 mM and pH = 7). The mixture then was incubated for 10 min in a water  
168 bath at  $30 \pm 1$  °C. The absorbance at  $\lambda = 420$  nm was measured to indicate the activity.

169 The concentrations of the protein solutions had been determined prior to the activity tests  
170 using the following equation:

$$171 \quad [Protein] = Abs_{280\text{ nm}}/E_{280\text{ nm}} \quad (1)$$

172 where  $[Protein]$  is the concentration of protein in the tested solution w/v%,  $Abs_{280\text{ nm}}$  is the  
173 absorbance of the tested protein solution at 280 nm, and  $E_{280\text{ nm}}$  is the absorbance of protein  
174 standard solution with concentration 0.05 w/v%. The concentrations of the solutions were diluted  
175 to be about 0.05 % w/v so as to give an absorbance value of less than 0.8. The activities of all  
176 samples were measured relative to that of a corresponding fresh sample, which was considered as  
177 the standard solution.

178

### 179 2.7. Inverse gas chromatography

180 IGC experiments were performed using an inverse gas chromatography (IGC 2000,  
181 Surface Measurement Systems Ltd., UK). A sample (~500 mg) was packed into a pre-silanised



182 glass column (300 mm × 3 mm i.d.). Three columns of each sample were analysed at 30 °C (the  
183 lowest temperature at which the IGC experiments can be performed to avoid thermal stress) and  
184 zero relative humidity, using anhydrous helium gas as the carrier. A series of n-alkanes (n-hexane  
185 to n-nonane) in addition to chloroform, as a monopolar electron acceptor probe ( $l_+$ ), and ethyl  
186 acetate, as a monopolar donor acceptor probe ( $l_-$ ), were injected through the columns at the infinite  
187 dilution region. Their retention times followed from detection using a flame ionization detector  
188 (FID).

189

### 190 2.7.1. Surface energy calculations

191 Our published methods were used to calculate the surface energies and verify their  
192 accuracy [17-19]. These methods describe the surface properties using the dispersive retention  
193 factor ( $K_{CH_2}^a$ ), the electron acceptor retention factor ( $K_{l_+}^a$ ), and the electron donor retention factor  
194 ( $K_{l_-}^a$ ), which are calculated using the retention times of probes:

$$195 \quad \ln(t_r - t_0) = (\ln K_{CH_2}^a) n + C \quad (2)$$

196 where n is the carbon number of the homologous n-alkanes,  $t_r$  and  $t_0$  are the retention times of the  
197 n-alkanes and a non-adsorbing marker, respectively,  $K_{CH_2}^a$  is the dispersive retention factor of the  
198 analysed powder and C is a constant. The linear regression statistics of equation 2 generate the  
199 value of  $t_0$  which gives its best linear fit. The slope of the equation 2 gives the value of  $K_{CH_2}^a$ .

$$200 \quad K_{l_+}^a = t_{nl+}/t_{nl+,ref} \quad (3)$$

$$201 \quad K_{l_-}^a = t_{nl-}/t_{nl-,ref} \quad (4)$$

202 where  $t_{nl+}$  and  $t_{nl+,ref}$  are the retention time of  $l_+$  and its theoretical n-alkane reference,  
 203 respectively,  $t_{nl-}$  and  $t_{nl-,ref}$  are the retention time of  $l_-$  and its theoretical n-alkane reference,  
 204 respectively.

$$205 \quad \ln t_{nl+,ref} = \ln t_{nCi} + \left( \frac{\alpha_{l+}(\gamma_{l+}^d)^{0.5} - \alpha_{Ci}(\gamma_{Ci}^d)^{0.5}}{\alpha_{CH_2}(\gamma_{CH_2})^{0.5}} \right) \ln K_{CH_2}^a \quad (5)$$

$$206 \quad \ln t_{nl-,ref} = \ln t_{nCi} + \left( \frac{\alpha_{l-}(\gamma_{l-}^d)^{0.5} - \alpha_{Ci}(\gamma_{Ci}^d)^{0.5}}{\alpha_{CH_2}(\gamma_{CH_2})^{0.5}} \right) \ln K_{CH_2}^a \quad (6)$$

207 where  $\alpha_{CH_2}$  and  $\gamma_{CH_2}$ ,  $\alpha_{Ci}$  and  $\gamma_{Ci}^d$ ,  $\alpha_{l+}$  and  $\gamma_{l+}^d$ , and  $\alpha_{l-}$  and  $\gamma_{l-}^d$  are the cross-sectional area and  
 208 the dispersive free energy of a methylene group, an n-alkane,  $l_+$  and  $l_-$ , respectively.  $t_{nCi}$  is the  
 209 retention time of the n-alkane.

210 The retention factors are then used to calculate the surface dispersive ( $\gamma_s^d$ ), electron donor ( $\gamma_s^-$ ) and  
 211 electron acceptor ( $\gamma_s^+$ ) components of the powders:

$$212 \quad \gamma_s^d = \frac{0.477 (T \ln K_{CH_2}^a)^2}{(\alpha_{CH_2})^2 \gamma_{CH_2}} \text{ mJ.m}^{-2} \quad (7)$$

$$213 \quad \gamma_s^- = \frac{0.477 (T \ln K_{l+}^a)^2}{(\alpha_{l+})^2 \gamma_{l+}^+} \text{ mJ.m}^{-2} \quad (8)$$

$$214 \quad \gamma_s^+ = \frac{0.477 (T \ln K_{l-}^a)^2}{(\alpha_{l-})^2 \gamma_{l-}^-} \text{ mJ.m}^{-2} \quad (9)$$

215 where  $\gamma_{l+}^+$  is the electron acceptor component of  $l_+$  and  $\gamma_{l-}^-$  is the electron donor component of  
 216  $l_-$ . The units of  $\alpha$  are  $\text{\AA}^2$  and of  $\gamma$  are  $\text{mJ.m}^{-2}$  in all equations.

217 The parameters of  $CH_2$  are calculated from the following equation:

$$218 \quad (\alpha_{CH_2})^2 \gamma_{CH_2} = -1.869T + 1867.194 \text{ \AA}^4 \cdot \text{mJ.m}^{-2} \quad (10)$$

219 The parameters of polar probes are still under debate and different values have been  
 220 reported [20-25]. In this paper, we used the values which were recently used for ethyl acetate ( $\gamma_{l-}^- =$

221 19.20 mJ/m<sup>2</sup>,  $\gamma_{l-}^d = 19.60$  mJ/m<sup>2</sup>,  $\alpha_{l-} = 48.0$  Å<sup>2</sup>) and for chloroform ( $\gamma_{l+}^+ = 3.80$  mJ/m<sup>2</sup>,  $\gamma_{l+}^d = 25.90$   
 222 mJ/m<sup>2</sup>,  $\alpha_{l+} = 44.0$  Å<sup>2</sup>) [17,22]. However, using any other different reported numbers will not  
 223 change the findings of the comparison.

224 The percentage coefficient of variation of  $\ln K_{CH_2}^a$  ( $\%CV_{\ln K_{CH_2}^a}$ ) is the indicator of the  
 225 accuracy of the surface energy measurements. The error of the slope of the equation 2 ( $SD_{\ln K_{CH_2}^a}$ )  
 226 is used to calculate  $\%CV_{\ln K_{CH_2}^a}$ :

$$227 \quad \%CV_{\ln K_{CH_2}^a} = \left( SD_{\ln K_{CH_2}^a} / \ln K_{CH_2}^a \right) \times 100 \quad (11)$$

228  $\%CV_{\ln K_{CH_2}^a}$  should be less than 0.7% to accept the accuracy of the measurement.  $\%CV_{\ln K_{CH_2}^a}$  is then  
 229 used to calculate the uncertainty range of  $\gamma_s^d$ :

$$230 \quad \text{Uncertainty Range of } \gamma_s^d = \left[ \left( \frac{100 \times \gamma_s^d}{100 + 7.5\% CV_{\ln K_{CH_2}^a}} \right) \text{ to } \left( \frac{100 \times \gamma_s^d}{100 - 7.5\% CV_{\ln K_{CH_2}^a}} \right) \right] \quad (12)$$

231

### 232 3. Results and discussion

#### 233 3.1. Microscopy

234 The photomicrographs of UNL, UNG, DeL, and DeG powders show that they had project-  
 235 area diameters of ~4 μm (Fig. S1), ~2.5 μm (Fig. S2), ~1.5 μm (Fig. S3), and ~1.5 μm (Fig. S4),  
 236 respectively. The particle sizes of the original powders were below 5 μm. Therefore, the attrition  
 237 mechanism was dominant during milling, and so the same original faces did not change [3].

238

#### 239 3.2. Differential scanning calorimetry (DSC)

240 For both proteins, DSC thermograms exhibited broad peaks ranging from ~30 to ~140 °C  
 241 (Figure 1). These peaks are due to water removal, and their areas depend on water residues in the

242 powders [3]. The enthalpy of the water evaporation peak was  $118\pm 11$ ,  $124\pm 6$ ,  $114\pm 9$  and  $130\pm 8$   
243 J/g for UNL, UNG, DeL, and DeG, respectively, and did not significantly change after milling (t-  
244 test:  $P < 0.05$ ). The protein powders exchange water with the surrounding air depending on  
245 conditions of temperature, relative humidity and exposure time. Therefore, the conditions used  
246 during milling did not change the water content of the powders. Also Figure 1 shows that the  
247 unprocessed proteins unfolded and a peak was detected at their apparent denaturation  
248 temperatures, which varied according to the protein. DSC thermograms of UNL displayed one  
249 denaturation peak at  $\sim 201$  °C, but UNG displayed two denaturation peaks at  $\sim 176$  °C and  $\sim 212$   
250 °C.  
251

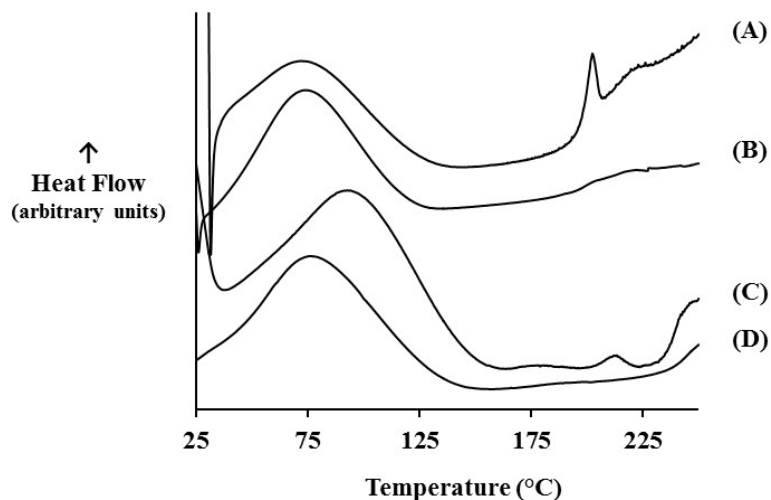


**Fig. 1.** Example DSC thermograms of protein powders (A) unprocessed lysozyme, (B) mechanically denatured lysozyme, (C) unprocessed  $\beta$ -galactosidase, (D) mechanically denatured  $\beta$ -galactosidase. Conditions: samples heated from 25 to 250 °C; heating rate: 10 °C/min.

---

252  
253 The difference in the thermal denaturation pattern can be due to the difference in the  
254 thermal unfolding mechanisms of the proteins. While lysozyme folds in a highly cooperative

255 manner and so exhibits an all-or-none thermal unfolding transition,  $\beta$ -galactosidase goes through  
256 a non-two state thermal unfolding transition resulting in two peaks [26,27]. The unfolding  
257 transition peaks were completely lost after mechanical denaturation. Hence there was no peak at  
258  $\sim 201$  °C for the milled lysozyme samples and neither were there peaks at  $\sim 176$  °C and  $\sim 212$  °C  
259 for the milled  $\beta$ -galactosidase. The complete disappearance of the unfolding transition peak from  
260 the DSC thermogram indicates the total transition of the protein from its folded state to its unfolded  
261 state [3].

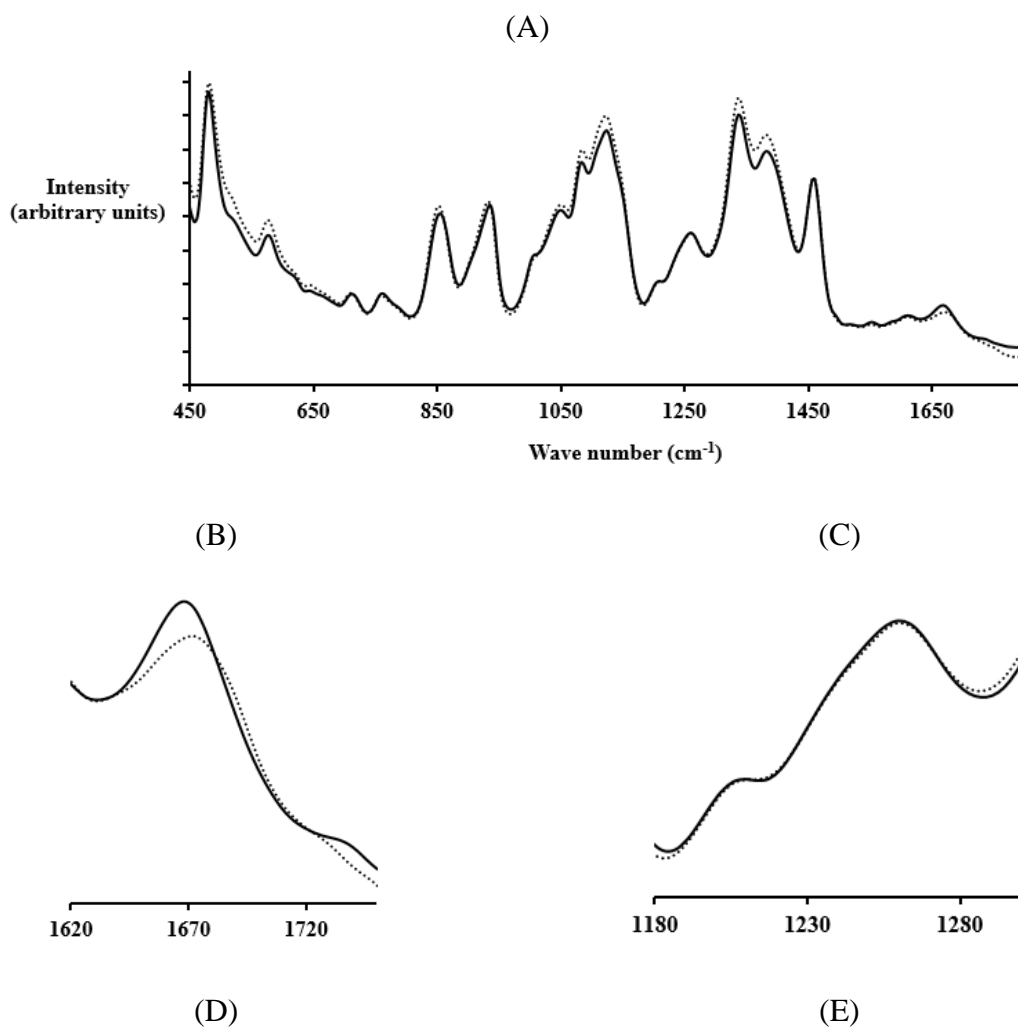
262

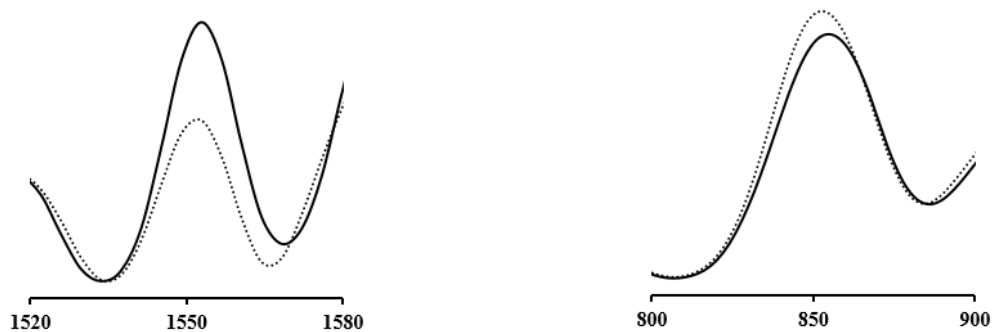
### 263 3.3. FT-Raman study

264 Raman spectroscopy was used to compare the molecular conformation of protein powders  
265 before and after mechanical denaturation. The band at  $\sim 1450$   $\text{cm}^{-1}$  indicates the CH bending  
266 vibrations of aliphatic side chains, and its intensity and position are unaffected by changes induced  
267 in protein structure after dehydration or applying different stresses [28]. Therefore, it was used as  
268 an internal intensity standard to normalize Raman spectra before comparison (Figures 2A and 3A).  
269 The vibration modes of amide I (C=O stretch) from  $1580$  to  $1720$   $\text{cm}^{-1}$  (Figures 2B and 3B) and  
270 amide III (N-H in-plane bend + C-N stretch) from  $1250$ – $1330$   $\text{cm}^{-1}$  (Figures 2C and 3C)  
271 demonstrated the secondary structure of  $\beta$ -galactosidase and lysozyme, respectively. The spectra  
272 of the denatured samples show that the modes of the amide I upshifted and broadened for both  
273 proteins, and the mode of the amide III intensified and downshifted, especially for lysozyme, but  
274 there was no change in the mode of amide III for  $\beta$ -galactosidase. These changes indicated the  
275 transformation of  $\alpha$ -helix content to  $\beta$ -sheets or a disordered structure which enhances the tendency  
276 of proteins to aggregate [3,29]. While  $\beta$ -galactosidase is a beta-type protein containing mainly  $\beta$ -

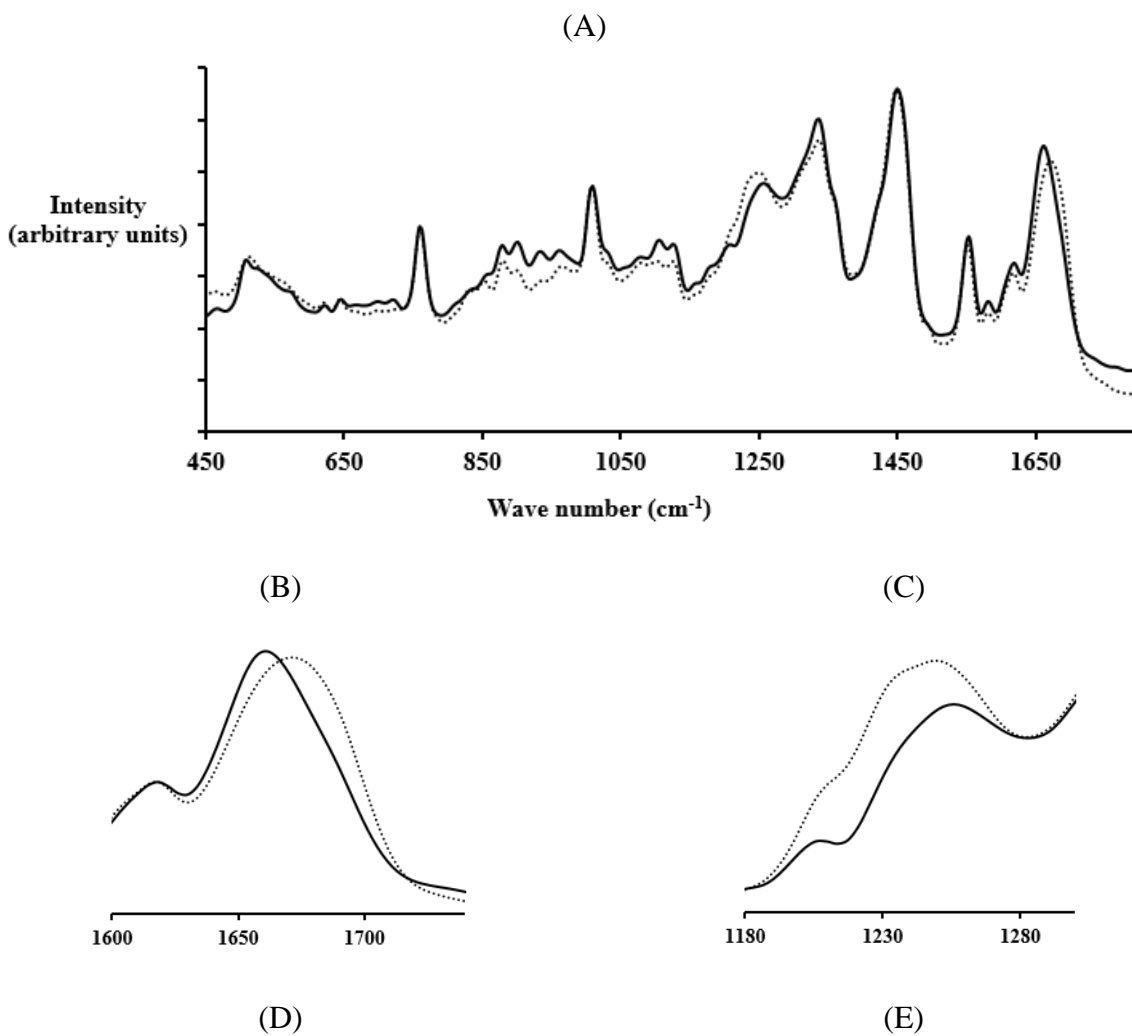
277 sheet structure and only 5%  $\alpha$ -helix [30], the secondary structure of lysozyme consists of 30%  $\alpha$ -  
278 helix [31]. This explains why no changes in the amide III of  $\beta$ -galactosidase were observed.

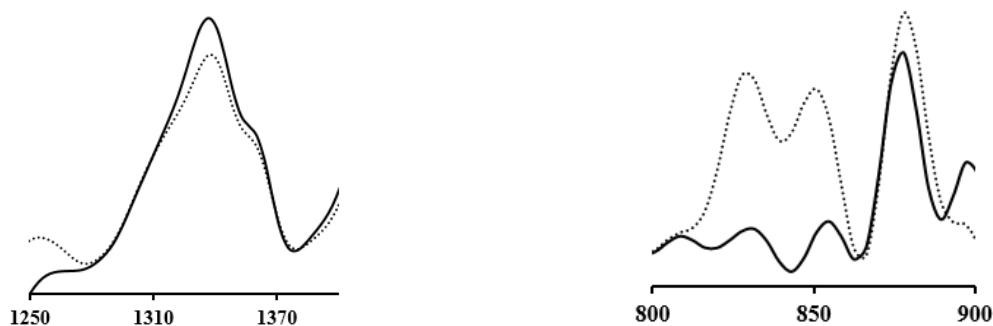
279 The aggregation of denatured proteins combined with changes in the vibration modes of of  
280 the aromatic residues at  $\sim 1550\text{ cm}^{-1}$  in  $\beta$ -galactosidase (Figure 2D),  $1320\text{-}1380\text{ cm}^{-1}$  in lysozyme  
281 (Figure 3D) and  $800\text{-}900\text{ cm}^{-1}$  in both proteins (Figures 2E and 3E). These changes in the vibration  
282 modes of the aromatic residues result from the changes in their micro-environment after  
283 denaturation because of their roles in the denaturation processes [29,32]. The aggregates of of  
284 denatured protein molecules are formed via  $\pi$ -stacking interactions of the aromatic residues [33].





285 **Fig. 2.** FT-Raman spectra of  $\beta$ -galactosidase powders, the unprocessed powders (solid lines) and  
 286 the mechanically denatured powders (dotted lines). Vibration modes of secondary structure are  
 287 (B) amide I and (C) amide III. Vibration modes of tertiary structure are (D) for Trp and (E) for Trp  
 288 and Tyr. The spectra were normalized using the methylene deformation mode at  $\sim 1450\text{ cm}^{-1}$  as an  
 289 internal intensity standard.  
 290



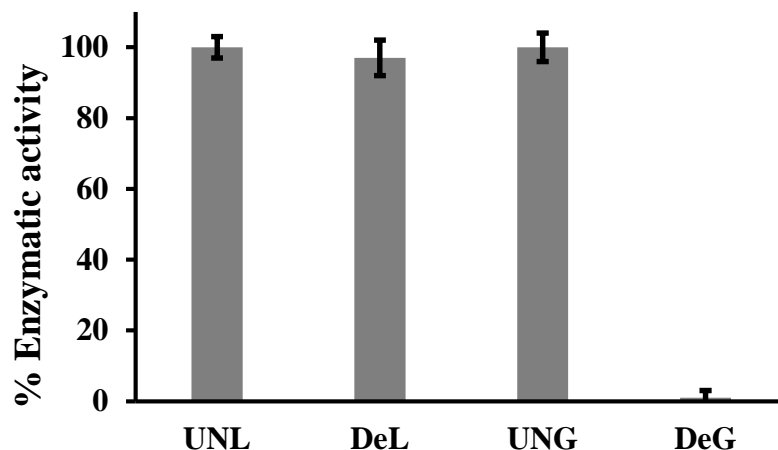


291 **Fig. 3.** FT-Raman spectra of lysozyme powders, the unprocessed powders (solid lines) and the  
 292 mechanically denatured powders (dotted lines). Vibration modes of secondary structure are (B)  
 293 amide I and (C) amide III. Vibration modes of tertiary structure are (D) for Trp and (E) for Trp  
 294 and Tyr. The spectra were normalized using the methylene deformation mode at  $\sim 1450\text{ cm}^{-1}$  as  
 295 an internal intensity standard.  
 296

### 297 3.4. Enzymatic assay

298 Therapeutic proteins may rapidly denature and lose their enzymatic activity. The structure  
 299 changes detected using FT-Raman and the absence of  $T_m$  detected by DSC have been used to  
 300 monitor the denaturation of proteins, and the results of Raman and DSC are linked to the results  
 301 of enzymatic activity [34]. Our DSC and Raman results confirmed the denaturation of both  
 302 proteins studied. The enzymatic assay showed that the mechanically denatured  $\beta$ -galactosidase  
 303 samples (DeG) demonstrated no enzymatic activity (Figure 4). However, the mechanically  
 304 denatured lysozyme samples (DeL) maintained full enzymatic activity when compared to an  
 305 unprocessed sample (t-test:  $P < 0.05$ ) (Figure 4). This is due to the ability of denatured lysozyme  
 306 to refold upon dissolution in aqueous media and thus the biological activity of lysozyme is fully  
 307 recovered following dissolution [3.35].  
 308





309  
310 **Fig. 4. Enzymatic activity of the unprocessed powders and the mechanically**  
311 **denatured powders of lysozyme and  $\beta$ -galactosidase.**  
312

313 *3.5. Surface free energy*

314 The IGC results (Table 1) confirm the acceptable accuracy of the IGC experiments  
315 considered in this work with  $\%CV_{\ln K_{CH_2}^a}$  values of less than 0.7% [18]. IGC data for the unprocessed  
316 powders demonstrated the differences in the surface free energy between  $\beta$ -galactosidase (an  
317 acidic protein) and lysozyme (a basic protein). UNG had higher  $\gamma_s^d$  compared to UNL because the  
318 uncertainty ranges of  $\gamma_s^d$  of UNG and UNL did not overlap for the three columns [18]. The surface  
319 acidity ( $\gamma_s^+$ ) and the surface basicity ( $\gamma_s^-$ ) of UNG were significantly different from their  
320 counterparts of UNL (t-test:  $P < 0.05$ ). The average of  $\gamma_s^+$  was  $16.2 \pm 0.2$  and  $12.4 \pm 0.1$   $\text{mJ} \cdot \text{m}^{-2}$  and  
321 the average of  $\gamma_s^-$  was  $5.5 \pm 0.2$  and  $10.5 \pm 0.6$   $\text{mJ} \cdot \text{m}^{-2}$  for UNG and UNL, respectively. This proves  
322 that UNG, chosen as a model for acidic proteins, has higher surface acidity and lower surface  
323 basicity compared to selected basic protein, UNL.

324  
325 **Table 1.** The surface energies ( $\gamma_s^d$ ,  $\gamma_s^+$  and  $\gamma_s^-$ ) and retention factors ( $K_{CH_2}^a$ ,  $K_{l+}^a$  and  $K_{l-}^a$ ) of the  
326 lyophilized lysozyme powder (UNL), the lyophilized  $\beta$ -galactosidase powder (UNG), the

327 mechanically denatured lyophilized lysozyme powder (DeL) and the mechanically denatured  
 328 lyophilized  $\beta$ -galactosidase powder (DeG).

Material	Column	$K_{CH_2}^a$	$K_{I^+}^a$	$K_{I^-}^a$	$\%CV_{\ln K_{CH_2}^a}$	$\gamma_s^d$ mJ.m <sup>-2</sup>	Uncertainty Range of $\gamma_s^d$ mJ.m <sup>-2</sup>	$\gamma_s^+$ mJ.m <sup>-2</sup>	$\gamma_s^-$ mJ.m <sup>-2</sup>
UNL	1	3.099	3.725	34.572	0.144	43.1	41.9-44.4	12.4	10.3
UNL	2	3.095	3.677	34.668	0.094	43.0	42.2-43.9	12.5	10.1
UNL	3	3.089	3.944	33.704	0.077	42.9	42.2-43.6	12.3	11.2
DeL	1	2.937	2.781	33.948	0.127	39.1	38.1-40.2	12.3	6.2
DeL	2	2.965	2.742	31.928	0.147	39.8	38.7-41.0	11.9	6.1
DeL	3	2.944	2.801	31.826	0.117	39.3	38.4-40.3	11.9	6.3
UNG	1	3.235	2.542	55.641	0.141	46.5	45.1-47.8	16.0	5.2
UNG	2	3.222	2.640	58.508	0.076	46.1	45.4-46.9	16.4	5.6
UNG	3	3.228	2.625	56.028	0.158	46.3	44.8-47.9	16.1	5.6
DeG	1	2.926	1.980	43.387	0.205	38.9	37.3-40.6	14.1	2.8
DeG	2	2.958	1.829	41.065	0.160	39.7	38.4-41.0	13.7	2.2
DeG	3	2.948	1.841	39.710	0.221	39.4	37.7-41.3	13.4	2.2

329

330 The isoelectric point (pI) of a protein indicates its relative acidity or basicity, the higher the  
 331 pI, the higher the basicity of the molecule [36]. The isoelectric points (pI) of the  $\beta$ -galactosidase  
 332 and lysozyme used are 4.6 and 11.3, respectively [13]. The molecule of  $\beta$ -galactosidase contains  
 333 ~11 w/w% basic amino acids (histidine, lysine, and arginine) and ~22 w/w% acidic (aspartic acid  
 334 and glutamic acid) residues [37], i.e., approximately double the number of acidic groups compared  
 335 to basic. Conversely the lysozyme contains ~18 w/w% and ~7 w/w% basic (histidine, lysine, and  
 336 arginine) and acidic (aspartic acid and glutamic acid) residues, respectively [38]. [Detailed](#)  
 337 [information regarding](#) the structures of  $\beta$ -galactosidase and lysozyme can be found in [37,38].  
 338 However, this is not the only determinant of energy as the surfaces of both the acidic (UNG) and  
 339 basic (UNL) protein powders were relatively basic (the values of  $\gamma_s^+ > \gamma_s^-$ ). Therefore to explain  
 340 our results further, the interaction of protein molecules with surfaces and interfaces, during  
 341 preparation using lyophilization technique, must be considered.

342 As protein molecules are surface active containing both polar and nonpolar groups, they  
 343 tend to adsorb to interfaces via hydrophobic interactions (London), coulombs (electrostatic) and/or

344 hydrogen bonding, and they reorient their surfaces to the parts which give the optimum attractive  
345 force and the most stable state (minimum energy) with a substrate or an interface [39]. Upon  
346 lyophilization, protein molecules adsorb to the formed ice via hydrophobic residues but not via  
347 hydrophilic residues, and this gives support to the hypothesis that the interaction of proteins with  
348 ice involves appreciable hydrophobic interactions [40]. The hydrophobic regions in protein  
349 molecules interact spontaneously with the ice faces by an entropy driving force [41]. The rich  
350 electron rings of aromatic residues orient so that the ring structures lie flat with the interface in  
351 order to maximize the interaction at interfaces and lower the Gibbs free energy of the system [42].  
352 Therefore, lyophilized protein particles expose the rich electron rings of the aromatic residues on  
353 their surfaces. Aromatic groups, via their  $\pi$  electrons, which are considered nucleophilic, can form  
354 hydrogen bonds with chemical groups (acidic polar probes) being the hydrogen donors [43].  
355 Therefore, exposing these rings to surfaces relatively increases their basicity compared to their  
356 acidity irrespective of the acidic or basic nature of the proteins themselves. Also the ring structures  
357 can participate in raising the dispersive surface energy via London interactions due to their high  
358 polarizability [43]. The aromatic residues (tryptophan, tyrosine, and phenylalanine) make up  
359 16% w/w of the  $\beta$ -galactosidase molecules and 14% w/w of the lysozyme molecules [37,38]. This  
360 explains the higher values of  $\gamma_s^d$  of  $\beta$ -galactosidase compared to lysozyme, prior to mechanical  
361 denaturation.

362 UNG was more acidic than UNL. The size and the shape of the molecule can also influence  
363 orientation. UNG is larger than UNL, with a globular shape and when some of the chemical groups  
364 are preferably exposed to a surface (energetically or entropically), this will expose not only those  
365 specific groups but also other closely associated groups which will vary in nature from one protein

366 to another.. Thus, the surfaces of the acidic protein ( $\beta$ -galactosidase) were more acidic compared  
367 to the basic protein (lysozyme).

368 Table 1 shows that mechanical denaturation decreased the dispersive free energy and the basicity  
369 of the surfaces of protein powders, irrespective of the nature of the protein (acidic or basic).  
370 Usually milling induces an increase in the dispersive energy due to the generation of surface  
371 amorphous regions or/and creation of higher energy crystal faces because of particle  
372 fracture/breakage, thus the surface acidity and basicity change according to the formation of new  
373 faces and regions [44,45]. However, in our case, due to lyophilization, the protein powders are  
374 amorphous with particle sizes below 5  $\mu\text{m}$ . Therefore, there would be no further size reduction by  
375 fracture mechanisms because of brittle ductile transition [3]. Therefore, the denatured protein  
376 powders were produced by milling where the attrition mechanism was dominant and so the same  
377 original faces did not change. During milling, the extensive mechanical energy completely  
378 denatured the protein molecules as confirmed by DSC and Raman results. This denaturation led to  
379 aggregation of the protein molecules via non-covalent interactions through  $\pi$ -stacking interactions  
380 [33]. This caused a loss of the aromatic groups, which are rich in  $\pi$  electrons, from the surfaces.  
381 Therefore, a decrease in the Van der Waals interactions, a major contributor to dispersive energy  
382 and nucleophilicity (basicity) occurred, and so  $\gamma_s^d$  and  $\gamma_s^-$  decreased after denaturation for both  
383 proteins. Also this loss of aromatic residues from the surface of the denatured powders renders  $\gamma_s^d$   
384 similar for both proteins. This is further evidence that the exposed aromatic residues raise the  $\gamma_s^d$   
385 as outlined previously. The Raman spectroscopic results confirmed that the aromatic residues were  
386 involved in the denaturation processes, therefore, supporting the findings and our interpretation of  
387 the IGC studies.

#### 388 **4. Conclusions**

389           The surface energies of the lyophilized protein powders differed according to their amino  
390 acid compositions. The absence of the thermal unfolding transition phase for the proteins  
391 (lysozyme and  $\beta$ -galactosidase) and the changes in the conformation of the back-bone and side  
392 chains confirmed that the mechanical milling process caused denaturation of the protein powders,  
393 and this denaturation could potentially be reversible in solution. The acidic protein powder ( $\beta$ -  
394 galactosidase) had higher surface acidity ( $\gamma_s^+$ ) and lower surface basicity ( $\gamma_s^-$ ) compared to the  
395 basic protein powder (lysozyme). However, both protein powders had relatively basic surfaces due  
396 to the rich electron rings of the aromatic residues which are nucleophilic. During mechanical  
397 denaturation, these rings tend to associate through  $\pi$ -stacking interactions and are thus concealed  
398 from the surface. Their removal reduced  $\gamma_s^-$  and  $\gamma_s^d$  of the surfaces of both protein powders, and  
399 thereby yielded similar  $\gamma_s^d$  for the surfaces of both proteins.

400

#### 401 **Acknowledgements**

402 MAM gratefully acknowledges CARA (Stephen Wordsworth and Ryan Mundy) the Universities  
403 of Bath and Bradford for providing academic fellowships.

404

#### 405 **Supplementary data**

406 Supplementary data associated with this article can be found, in the online version, at  
407 <http://dx.doi.org/XXXX>.

408

409

410

411

412

413 **References**

414 [1] H. Hoyer, W. Schlocker, K. Krum, A. Bernkop-Schnürch, *Eur. J. Pharm. Biopharm.* 69 (2008)  
415 476.  
416 [2] W. Schlocker, S. Gschliesser, A. Bernkop-Schnürch, *Eur. J. Pharm. Biopharm.* 62 (2006) 260.  
417 [3] M.A. Mohammad, I.M. Grimsey, R.T. Forbes, *J. Pharm. Biomed. Anal.* 114 (2015) 176.  
418 [4] W. He, K. Yang, L. Fan, Y. Lv, Z. Jin, S. Zhu, C. Qin, Y. Wang, L. Yin, *Int. J. Pharm.* 495  
419 (2015) 9.  
420 [5] R. Caillard, M. Subirade, *Int. J. Pharm.* 437 (2012) 130.  
421 [6] V. Karde, C. Ghoroi, *Int. J. Pharm.* 475 (2014) 351.  
422 [7] X. Han, L. Jallo, D. To, C. Ghoroi, R. Davé, *J. Pharm. Sci.* 102 (2013) 2282.  
423 [8] D. Cline, R. Dalby, *Pharm. Res.* 19 (2002) 1274.  
424 [9] M.S. Killian, H.M. Krebs, P. Schmuki, *Langmuir* 27 (2011) 7510.  
425 [10] O. Planinsek, A. Trojak, S. Srcic, *Int. J. Pharm.* 221 (2001) 211.  
426 [11] Y. Hirakura, H. Yamaguchi, M. Mizuno, H. Miyanishi, S. Ueda, S. Kitamura, *Int. J. Pharm.*  
427 340 (2007) 34.  
428 [12] Q. Husain, *Crit. Rev. Biotechnol.* 30 (2010) 41.  
429 [13] M. Ospinal-Jiménez, D.C. Pozzo, *Langmuir* 28 (2012) 17749.  
430 [14] R.R. Haj-Ahmad, A.A. Elkordy, C.S. Chaw, A. Moore, *Eur. J. Pharm. Sci.* 49 (2013) 519.  
431 [15] S. Chakraborti, T. Chatterjee, P. Joshi, A. Poddar, B. Bhattacharyya, S.P. Singh, V. Gupta, P.  
432 Chakrabarti, *Langmuir* 26 (2010) 3506.  
433 [16] R.E. Hamlin, T.L. Dayton, L.E. Johnson, M.S. Johal, *Langmuir* 23 (2007) 4432.  
434 [17] M.A. Mohammad, *J. Chromatogr. A* 1318 (2013) 270.  
435 [18] M.A. Mohammad, *J. Chromatogr. A* 1399 (2015) 88.  
436 [19] M.A. Mohammad, *J. Chromatogr. A* 1408 (2015) 267.  
437 [20] B. Shi, D. Qi, *J. Chromatogr. A* 1231 (2012) 73.  
438 [21] C. Della Volpe, D. Maniglio, M. Brugnara, S. Siboni, M. Morra, *J. Colloid Interface Sci.* 271  
439 (2004) 434.  
440 [22] S.C. Das, I. Larson, D.A. Morton, P.J. Stewart, *Langmuir* 27 (2011) 521.  
441 [23] C.D. Volpe, S. Siboni, *J. Colloid Interface Sci.* 195 (1997) 121.  
442 [24] J. Schultz, L. Lavielle, C. Martin, *J. Adhesion* 23 (1987) 45.  
443 [25] C.J. Van Oss, R.J. Good, M.K. Chaudhury, *Langmuir* 4 (1988) 884.  
444 [26] B. Maroufi, B. Ranjbar, K. Khajeh, H. Naderi-Manesh, H. Yaghoubi, *Biochim. Biophys. Acta*  
445 1784 (2008) 1043.  
446 [27] J.M. Sánchez, V. Nolan, M.A. Perillo, *Colloids Surf. B Biointerfaces* 108 (2013) 1.  
447 [28] T.J. Yu, J.L. Lippert, W.L. Peticolas, *Biopolymers* 12 (1973) 2161.  
448 [29] E.N. Lewis, W. Qi, L.H. Kidder, S. Amin, S.M. Kenyon, S. Blake, *Molecules* 19 (2014)  
449 20888.  
450 [30] S.R. Tello-Solís, J. Jiménez-Guzmán, C. Sarabia-Leos, L. Gómez-Ruíz, A.E. Cruz-Guerrero,  
451 G.M. Rodríguez-Serrano, M. García-Garibay, *J. Agric. Food Chem.* 53 (2005) 10200.  
452 [31] P.J. Artymiuk, C.C.F. Blake, D.W. Rice, K.S. Wilson, *Acta Crystallogr. B: Struct.*  
453 *Crystallogr. Cryst. Chem.* B38 (1982) 778.  
454 [32] C. Zhou, W. Qi, E.N. Lewis, J.F. Carpenter, *Anal. Biochem.* 472 (2015) 7.  
455 [33] S. Jang, J. Jang, W. Choe, S. Lee, *ACS Appl. Mater. Interfaces* 7 (2015) 1250.  
456 [34] A. Torreggiani, M. Di Foggia, I. Manco, A. De Maio, S.A. Markarian, S. Bonora, *J. Mol.*  
457 *Struct.* 891 (2008) 115.

- 458 [35] A. Torreggiani, M. Tamba, I. Manco, M.R. Faraone-Mennella, C. Ferreri, C. Chatgialoglu,  
459 J. Mol. Struct. 744 (2005) 767.
- 460 [36] C. Sun, J.C. Berg, Adv. Colloid Interface Sci. 105 (2003) 151.
- 461 [37] Y. Tanaka, A. Kagamiishi, A. Kiuchi, T. Horiuchi, J. Biochem. 77 (1975) 241.
- 462 [38] M.C. Vaney, S. Maignan, M. Riès-Kautt, A. Ducriux, Acta Crystallogr. D. Biol. Crystallogr.  
463 52 (1996) 505.
- 464 [39] C. Chaiyasut, Y. Takatsu, S. Kitagawa, T. Tsuda, Electrophoresis 22 (2001) 1267.
- 465 [40] J. Baardsnes, P.L. Davies, Biochim Biophys Acta. 160 (2002) 49.
- 466 [41] S. Pezennec, F. Gauthier, C. Alonso, F. Graner, T. Croguennec, G. Brulé, A. Renault, Food  
467 Hydrocolloids 14 (2000) 463.
- 468 [42] M. Jurkiewicz-Herbich, A. Muszalska, R. Słojkowska, Colloids Surfaces A: Physicochem.  
469 Eng. Aspects 131 (1998) 315.
- 470 [43] G.I. Makhatadze, P.L. Privalov, Biophys. Chem. 50 (1994) 285.
- 471 [44] U.V. Shah, Z. Wang, D. Olusanmi, A.S. Narang, M.A. Hussain, M.J. Tobby, J.Y. Heng, Int.  
472 J. Pharm. 495 (2015) 234.
- 473 [45] X. Han, L. Jallo, D. To, C. Ghoroi, R. Davé, J. Pharm. Sci. 102 (2013) 2282.